XFEL.EU TR-2013-002

TECHNICAL REPORT

Estimates of the Fluorescence-Induced Backscattered Dose for the LPD Detector

December 2013

S. Hauf and A. Koch
for the Detector Development group (WP75)
at European XFEL

European X-Ray Free-Electron Laser Facility GmbH
Albert-Einstein-Ring 19
22761 Hamburg
Germany

Contents

Introduction

This report gives an estimate of the additional dose, or photons, the Large Pixel Detector (LPD) will be subjected to because of fluorescence and backscattered radiation emitted by the tantalum layer shielding the application-specific integrated circuits (ASICs). The Geant4-based [Agostinelli, et al., 2003; Amako, et al., 2006] Mulassis simulation environment [Lei, et al., 2002] used to obtain these results is also described.

Overview

The LPD sensor is positioned directly on top of the front-end electronic ASICs, resulting in a sandwiched structure, as shown in Figure 1. To shield the ASICs from ionizing radiation passing through the sensor, it is foreseen to include a 0.25 mm or 0.5 mm thick tantalum or tungsten layer between these two components. This layer will not be homogeneous across the detector area, as the pixels and the ASICs are connected by silicon interposers.

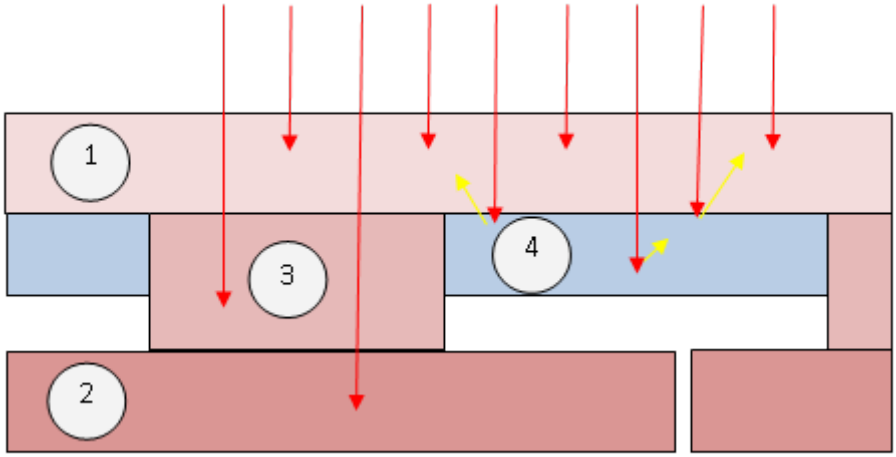

Figure 1. *Schematic of the area near the LPD sensitive area of the 32 x 16 pixel basic detector module (1). The ASICs (2), interposers (3), and tantalum/tungsten shielding (4) are shown. X-rays hitting the detector are shown in red, and fluorescence emission is shown in yellow.*

Subjecting the tantalum/tungsten to ionizing radiation excites individual atoms within the layer, in turn resulting in the emission of fluorescence radiation (see Table 1 and Table 2 for an overview). Additionally, backscattering of the incident radiation will occur. In the worst case, this emission manifests itself in an inhomogeneous background, which is modulated in accordance with the presence of tantalum/tungsten structures below the pixels. Different works have demonstrated that the effect can be simulated with Geant4-based Monte-Carlo simulations and can thus be taken into account during detector design [Hauf, 2012; Tenzer, et al., 2008].

For a first estimate of the effect of fluorescence on the LPD background, a very simplified simulation using the Geant4-based Mulassis tool was done. After a short description of the simulation approach in Chapter 1, “Mulassis simulations”, the results are described in Section 2.1, “Influence of fluorescence on detector background (energy view)”, and Section 2.3, “Dose–layer thickness dependency”.

Table 1. *X-ray emission energies of tantalum as given in [Thompson & Vaughan, 2009]. The shaded area indicates emission of relevance for LPD.*

	$K\alpha_1$	$K\alpha_2$	$K\beta_1$	$L\alpha_1$	$L\alpha_2$	$L\beta_1$	$L\beta_2$	$L\gamma_1$	$M\alpha_1$
E [keV]	57.532	56.277	65.223	8.146	8.087	9.343	9.651	10.895	1.710

Table 2. *X-ray emission energies of tungsten as given in [Thompson & Vaughan, 2009]. The shaded area indicates emission of relevance for LPD.*

	$K\alpha_1$	$K\alpha_2$	$K\beta_1$	$L\alpha_1$	$L\alpha_2$	$L\beta_1$	$L\beta_2$	$L\gamma_1$	$M\alpha_1$
E [keV]	59.318	57.981	67.244	8.397	8.335	9.672	9.961	11.295	1.775

1 Mulassis simulations

For a first estimate of the magnitude of the expected fluorescence emission, a detailed detector model is not required. Accordingly, a simplified simulation geometry, consisting of planar slabs with thicknesses equivalent to the individual components, was used. A sketch of this geometry is shown in Figure 2. To minimize development time, the well-tested Mulassis tool, which is based on Geant4.9.3, was used. This tool allows for the definition of such geometries using simple macro commands, and supports the output of, for example, received dose and pulse height spectra for each layer.

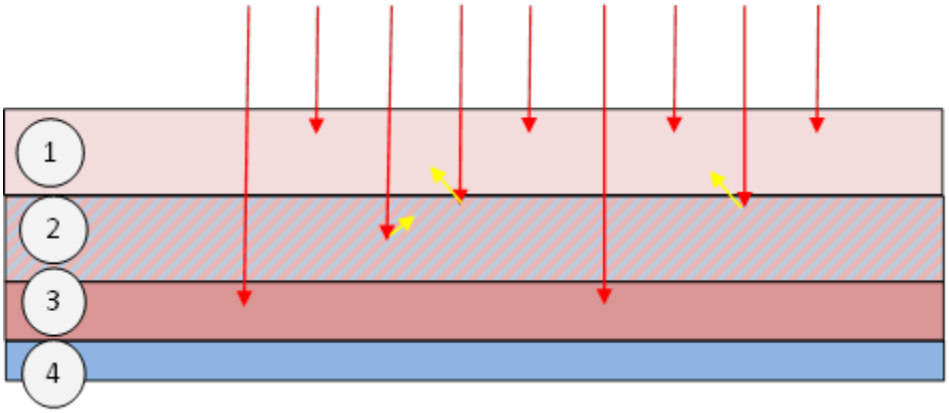

Figure 2. *A sketch of the Mulassis simulation geometry. The sensitive area (1) of silicon is followed by either a tantalum, tungsten, or silicon layer (2) resembling the shielding or interposer, another silicon layer modelling the ASIC (3), and finally a molybdenum carrier (4).*

To investigate the influence of the thickness of the tantalum layer on both the amount of (additional) fluorescence emission hitting the sensitive area and the dose deposited in the ASIC, simulations with varying tantalum thicknesses between 10 µm and 500 µm were run for X-ray energies of 12 keV and 20 keV. For each of these simulations, at least 10 million primary X-rays were emitted perpendicularly onto the sensitive area, assuring sufficient statistics. The approximation of simulating only radiation impacting perpendicular to the detector should be valid for most experimental scenarios.

For the LPD with its large pixels, charge sharing is not expected to have a considerable effect.

The simulations described above were run using the “leem” option of Mulassis, thus enabling the Geant4 low-energy electromagnetic physics processes, which include the simulation of fluorescence emission and Auger electrons.

2 Results

2.1 Influence of fluorescence on detector background (energy view)

As a first step, pulse height spectra (PHS) of the simulated layers were obtained in order to verify the correct production of fluorescence emission both for the baseline thickness tantalum (500 µm) and tungsten (205 µm) layers. Figures 3 to 7 show these spectra normalized to the number of events—that is, photons—registered at a given energy for each primary X-ray emitted onto the detector.

It is apparent from Figures 3 to 7 that the Mulassis simulation correctly produces the fluorescence emission. The ~ 0.4 events registered at the primary photon energy of 12 keV and 20 keV correspond well to the respective quantum efficiencies for 500 µm of silicon determined e.g. for a 450 µm thick pnCCD in [Meidinger, et al., 2010] for these energies. The fluorescence yields are lower than those given for example in [Thompson & Vaughan, 2009] due to self-absorption of the emission in the tantalum or tungsten layers.

To get an estimate on the number of events per photon registered on the detector without the occurrence of fluorescence emission, a simulation was run in which the shielding was replaced by a 500 µm thick silicon layer. It is apparent from Figures 3 to 7 that the event numbers below the incident photon energy are lower by up to two orders of magnitude. The addition of extra layers of copper and tin, acting as a graded-Z shielding, was also investigated (Figure 7). The addition of such layers can shift the fluorescence to lower energies, which, depending on the energy threshold settings (i.e. the energy above which a fluorescence event with a lower energy than the beam energy will still be considered an event), might be advantageous.

The number of fluorescence photons impeding the detector background depends on the flux and on the threshold energy. Accordingly, the higher the flux and the lower the threshold energy, the more fluorescence photons will register as background events. One should note, however, that simply setting the threshold energy high is not an optimal solution, as this will also reject true events that registered as split events in multiple pixels.

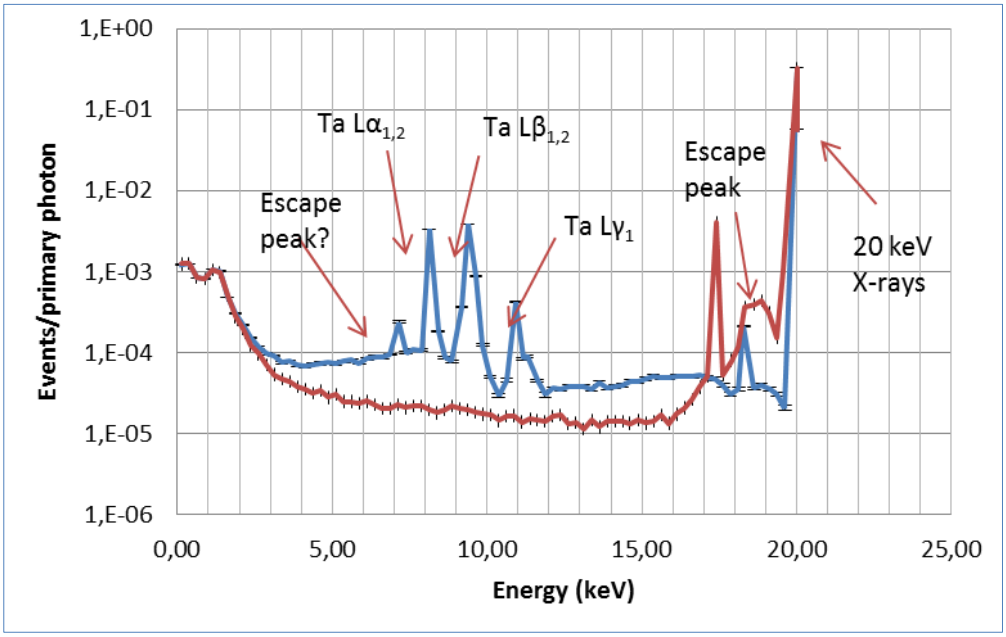

Figure 3. *Simulated pulse height spectrum registered in a 500 µm silicon detector with an underlying 500 µm tantalum shield when irradiated by 20 keV X-rays (blue). As a reference, a PHS where the tantalum is replaced by 500 µm of silicon is shown (red). The spectrum has been normalized to events per primary X-ray photon.*

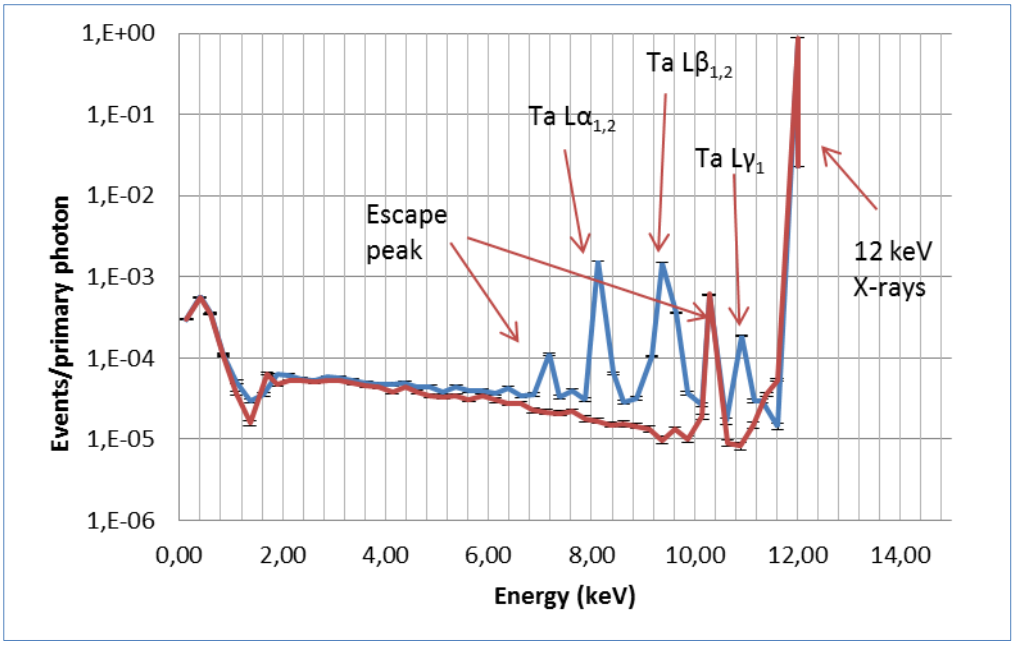

Figure 4. *Simulated pulse height spectrum registered in a 500 µm silicon detector with an underlying 500 µm tantalum shield when being irradiated by 12 keV X-rays (blue). As a reference, a PHS where the tantalum is replaced by 500 µm of silicon is shown (red). The spectrum has been normalized to events per primary X-ray photon.*

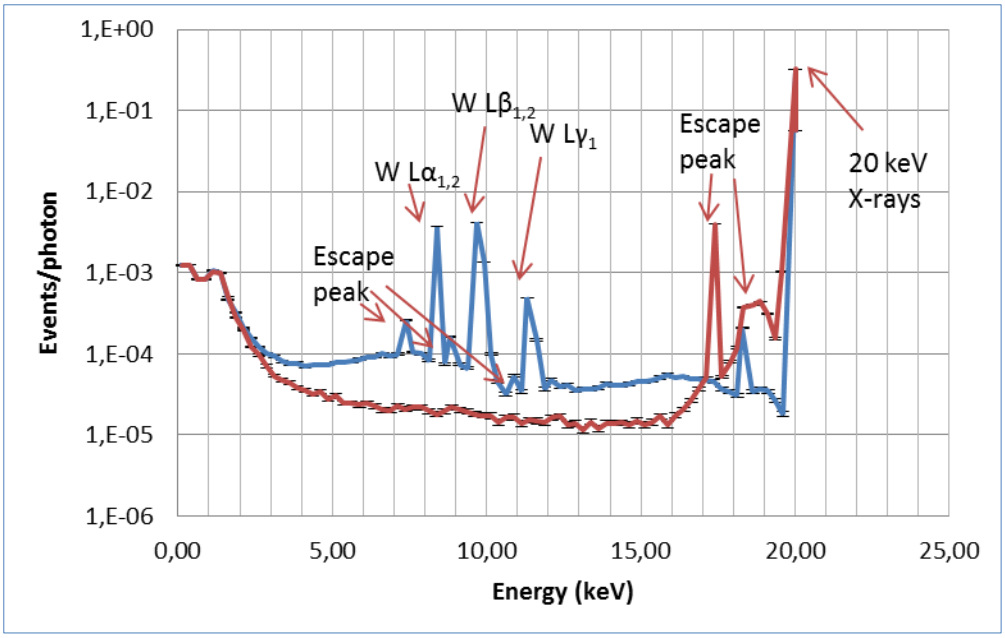

Figure 5. *Simulated pulse height spectrum registered in a 500 µm silicon detector with an underlying 205 µm tungsten shield when being irradiated by 20 keV X-rays (blue). As a reference, a PHS where the tungsten is replaced by 500 µm of silicon is shown (red). The spectrum has been normalized to events per primary X-ray photon.*

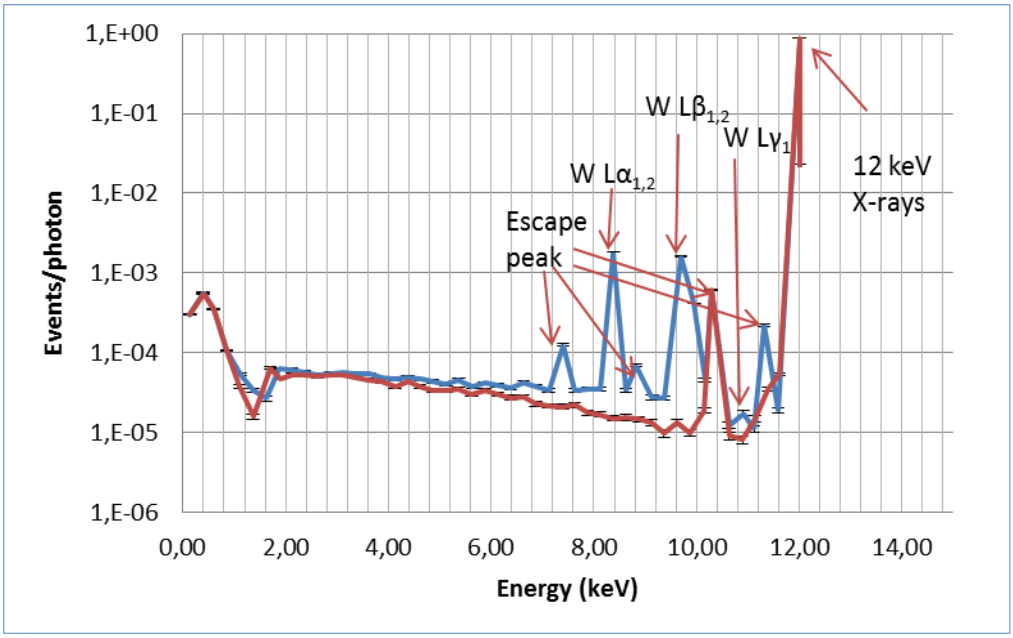

Figure 6. *Simulated pulse height spectrum registered in a 500 µm silicon detector with an underlying 205 µm tungsten shield when being irradiated by 12 keV X-rays (blue). As a reference, a PHS where the tungsten is replaced by 500 µm of silicon is shown (red). The spectrum has been normalized to events per primary X-ray photon.*

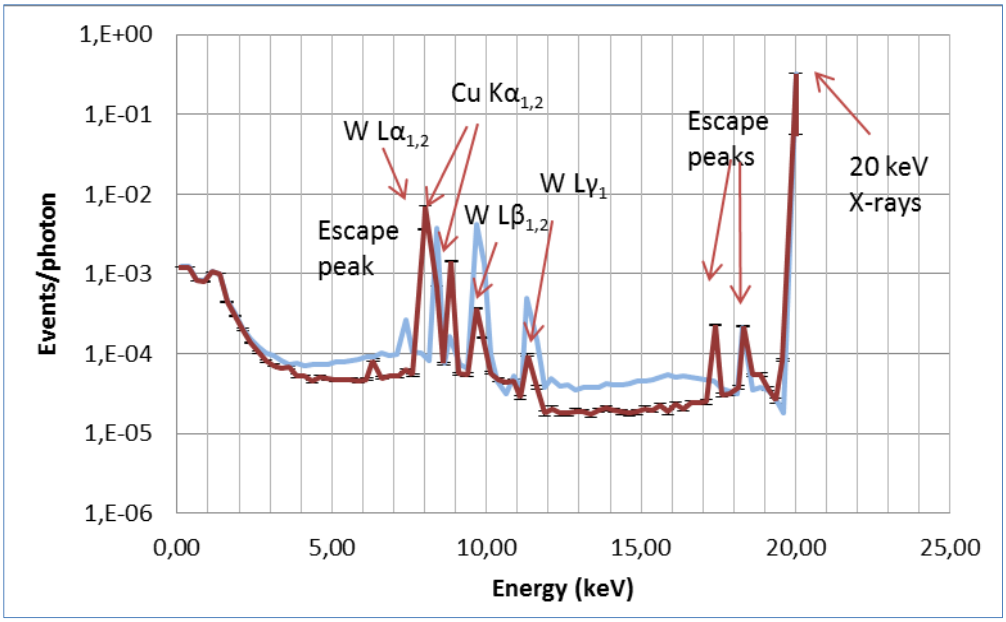

Figure 7. *Simulated pulse height spectrum registered in a 500 µm silicon detector with an underlying 105 µm tungsten shield and 50 µm copper and tin layers when being irradiated by 20 keV X-rays (blue). As a reference, a PHS where only a tungsten layer is present is shown (red). The spectrum has been normalized to events per primary X-ray photon.*

The number of fluorescence photons will follow Poisson statistics. Accordingly, the presence of fluorescence photons will introduce an additional uncertainty on top of the Poisson error of the incident radiation. Figure 8 shows the dependency of this additional uncertainty, expressed as a fraction of the Poisson error for different threshold scenarios and primary photon counts. As both uncertainties scale with the root of the photon number, the constant behaviour shown in the figure is to be expected. As a result, the additional uncertainty will only depend on if and how fluorescence emission will be treated as valid events (a selection of possibilities is given in the figure). In terms of relative uncertainty of the photon number, i.e. $(\sqrt{n_{fluor}})/n_{incident}$, even for very low photon numbers, the maximum fluorescence-induced uncertainty is below 0.9% (Figure 9).

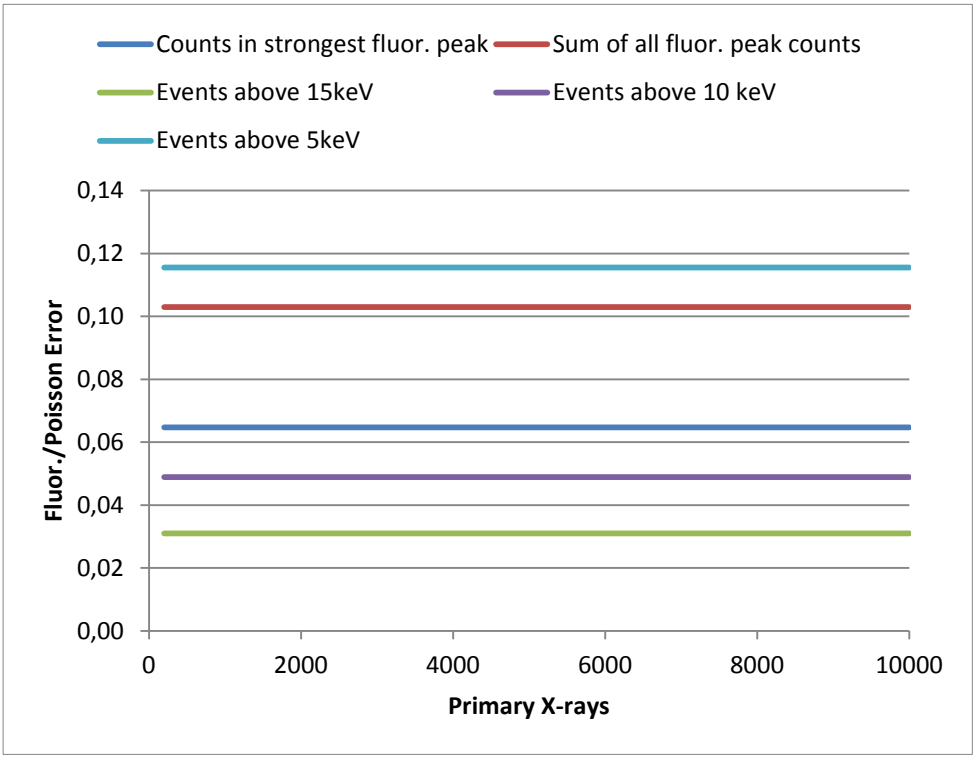

Figure 8. *Fraction of the fluorescence-related uncertainty with respect to the Poisson uncertainty for a given number of primary X-ray photons*

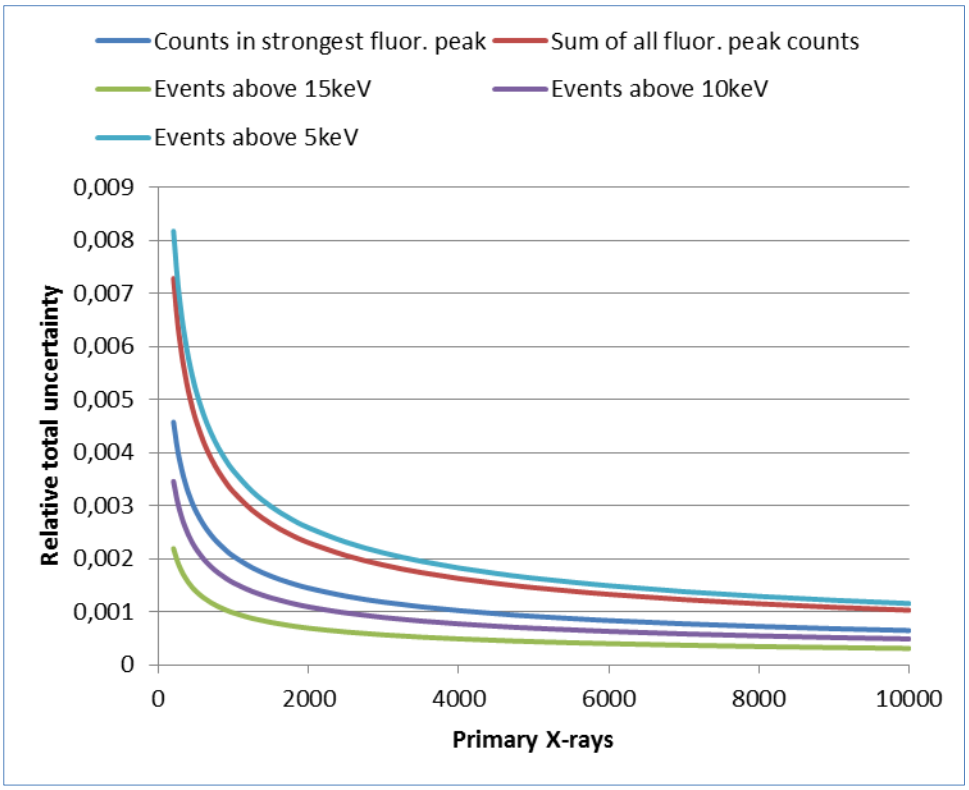

Figure 9. *Relative fluorescence-induced uncertainty with respect to primary X-ray photons*

As a final verification, analytical calculations, which took into account backscattering and fluorescence, were done (Table 3). The Monte-Carlo simulations and analytical calculations agree within a factor of 2 and yield the same general trend of the fluorescence emission from the tungsten shielding, with an order of magnitude higher intensity, than the backscattering from the silicon interposer. This is a reasonable agreement considering the absence of self-absorption and scattering in the analytical solution.

Table 3. *Results from analytical approximation of silicon and tungsten fluorescence and backscattering*

Material	Si (12 keV)	Si (20 keV)	W (12 keV)	W (20 keV)
Backscattering	4.067E-3	2.503E-3	2.610E-3	1.779E-3
Fluorescence	2.869E-4	6.113E-5	4.476E-2	1.489E-2

Backsc. (W/Si)	0.64	0.71
Fluor. (W/Si)	156.02	243.65
Total (W/Si)	**10.87**	**6.50**

The absolute magnitude of fluorescence emission is of lesser importance, as it will result only in a higher gain for individual pixels, something that can be corrected for during calibration. Accordingly, it is unlikely that the background will be significantly inhomogeneous due to underlying detector structures.

The findings based on the Mulassis results have been confirmed by a hand-tailored Geant4 simulation, which investigated the radiation passing from the shielding or interposer layer back into the sensor. The fluorescence intensity from the tungsten is approximately one order of magnitude higher than the backscattering intensity from the silicon interposer. If the radiation is weighted by its energy, this divergence vanishes in correspondence with the Mulassis results.

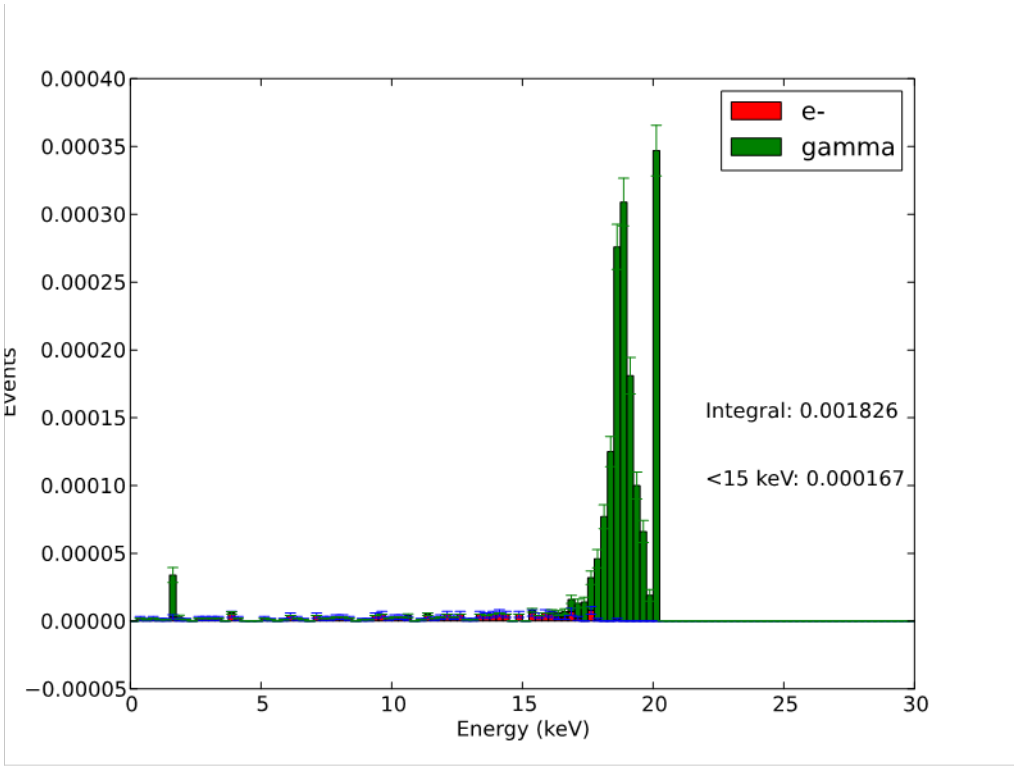

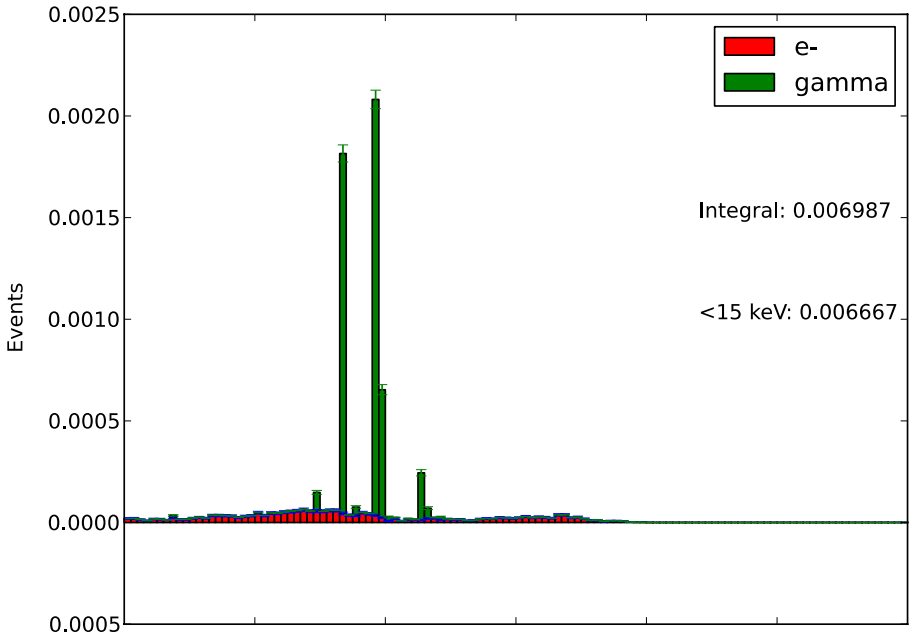

Figure 10. *Radiation incident from the shielding or interposer onto the sensitive detector area for a tungsten shielding (top panel) and the silicon interposer (bottom panel). Note that the y-axes have differing scales.*

2.2 Influence on detector gain (intensity view)

The previous section focused on the influence of the fluorescence emission in an energy-dependent way. From a simulation perspective, this has the benefit of easily allowing us to check for the presence of emission at the appropriate energies and to investigate the influence of individual emission lines. The LPD is not energy-sensitive though; it will measure photon intensities and, in first order, all photons are assumed to have the same energy—that of the X-ray beam.

As has been shown in the previous section, the mono-energetic nature of the photons registered in the detector is not realistic, especially if underlying high-Z layers such as tantalum or tungsten are present. Instead, additional fluorescence photons at lower energies will also add to the registered signal. This is reflected in a higher gain for the pixels lying above such a layer. The magnitude of this gain variation can be calculated in a first approximation by comparing the total number of "events" registered in the detector per incident X-ray for pixels with and without shielding layers.

In second order, it can be further taken into account that fluorescence energies lower than the incident X-ray energy count only a fraction towards a "full photon", accordingly the events per channel are weighted E_{ch}/E_{in}, with E_{ch} and E_{in} being the energies of the fluorescence and the incident photon in the energy picture presented in Section 2.1, "Influence of fluorescence on detector background (energy view)".

Table 4 shows the relative gain changes for pixels above a shielding layer when compared to pixels above a silicon interposer. It is apparent from the tables that the additional gain from the shielding-induced fluorescence is counterbalanced by the backscattering occurring in the silicon, which results in photons at an escape peak energy of

$E_{ch} = E_{in} - E_{k\alpha}$, with $E_{K\alpha} = 1.739$ keV.

Especially if the weighting is taken into account, this backscattering leads to a small increase in gain for the non-shielded pixels.

The energy thresholds given in the tables are of interest for very low photon counts. For high photon counts, the different photon energies of the incident X-ray, backscattered X-ray, and fluorescence photon are accounted for by the gain, which includes the mean number of “secondary” photons that are to be expected. Instead, a single photon may register as the analogue-to-digital unit (ADU) value corresponding to the incident energy of the X-ray (i.e. the X-ray is absorbed in the sensor) or a lower ADU value (i.e. the X-ray passes through the sensor and is backscattered at a lower energy, or it is absorbed in the shielding layer and a resulting fluorescence photon of lower energy is detected).

This behaviour is not problematic if the ADU value corresponding to the lowest energy of the fluorescence emission is well above the maximum ADU value that is regarded as background noise. In such a scenario, even low ADU values can still be distinguished as photon signals (i.e. it does not matter if the incident X-ray, a backscattered X-ray, or one or many fluorescence photons are detected as a signal). The situation is more problematic when noise threshold ADU and lowest possible fluorescence ADU overlap. Then the signal cannot be clearly attributed to the photon anymore but may also be noise. Accordingly, a photon event is then only defined by its probability.

This should be kept in mind for experiments that will detect very low photon counts.

Table 4. *Relative change of gain in per cent for a 20 keV photon incident on a pixel above a shielding layer compared to the gain of a pixel above an interposer. The uncertainties are generally below 0.4%.*

Material		Full	>5 keV	>15 keV	Incident
Tantalum	Simple	101.14	101.05	98.32	99.91
	Weighted	99.71	99.69	98.46	99.91
Tungsten	Simple	101.40	101.30	98.32	99.92
	Weighted	99.86	99.84	98.46	99.92

2.3 Dose–layer thickness dependency

The primary motivation for the addition of a tantalum or tungsten layer is to limit the radiation dose received by the underlying ASIC. This shielding's thickness should be minimized so that it still effectively protects the ASIC but does not result in the production of unnecessary fluorescence emission.

Two collections of simulations were run: one for a tantalum layer with the detector irradiated with 12 keV X-rays, and one for a tungsten layer where the detector was irradiated with 20 keV X-rays. Each of the simulations consisted of 50 million X-rays emitted perpendicularly onto the entrance window side of the detector; the X-ray flux was set at 10^{15} photons/cm²/s, which corresponds to about 1 year of beam time for the LPD.

Figures 11 and 12 show the dose registered in the individual layers in dependence of the tantalum or tungsten layer thickness. It is apparent from the figures that the ASIC is well shielded from radiation if the layer thickness is above ~ 125 µm.

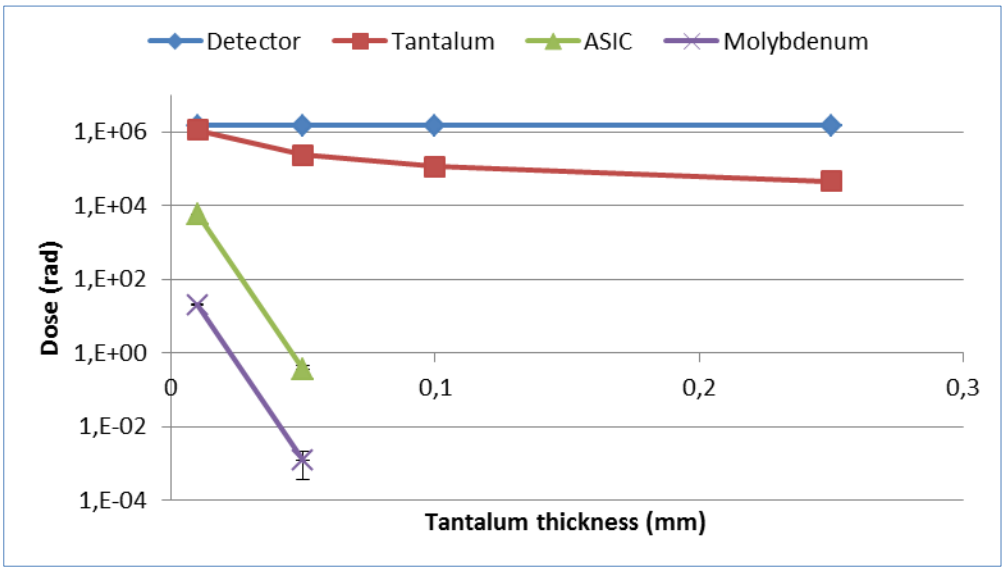

Figure 11. *Radiation dose from 12 keV X-rays accumulated in different components. For tantalum thicknesses above 100 µm, the simulations resulted in no registered dose in the ASIC or underlying molybdenum.*

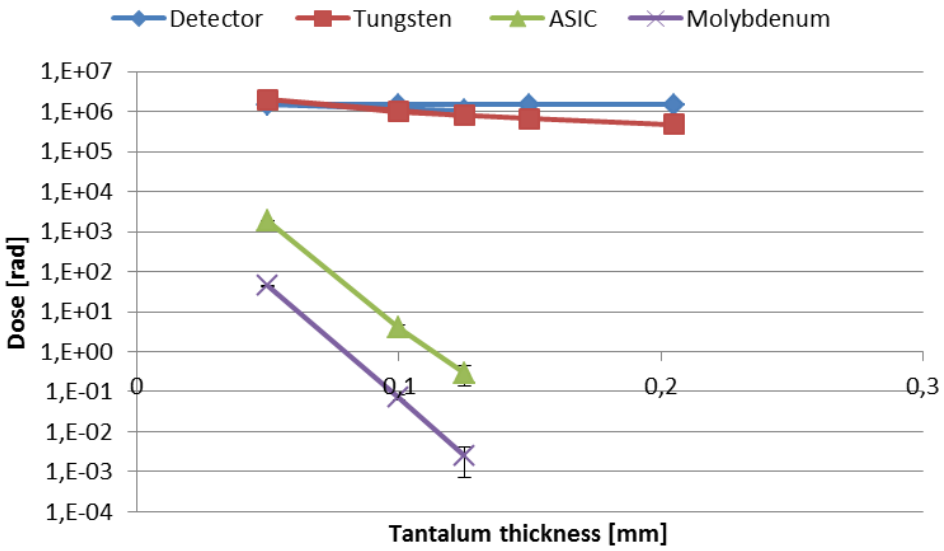

Figure 12. *Radiation dose from 20 keV X-rays accumulated in different components. For tungsten thicknesses above 125 µm, the simulations resulted in no registered dose in the ASIC or underlying molybdenum.*

Finally, Figure 13 shows the dose deposited in the ASIC if only silicon is present above, which may for example be the case for the interconnects. Again the dose is shown as a function of layer thickness. Here, a dose greater than 100 000 rad = 1 kGy has to be expected for the simulated flux of 10^{15} photons/cm²/s.

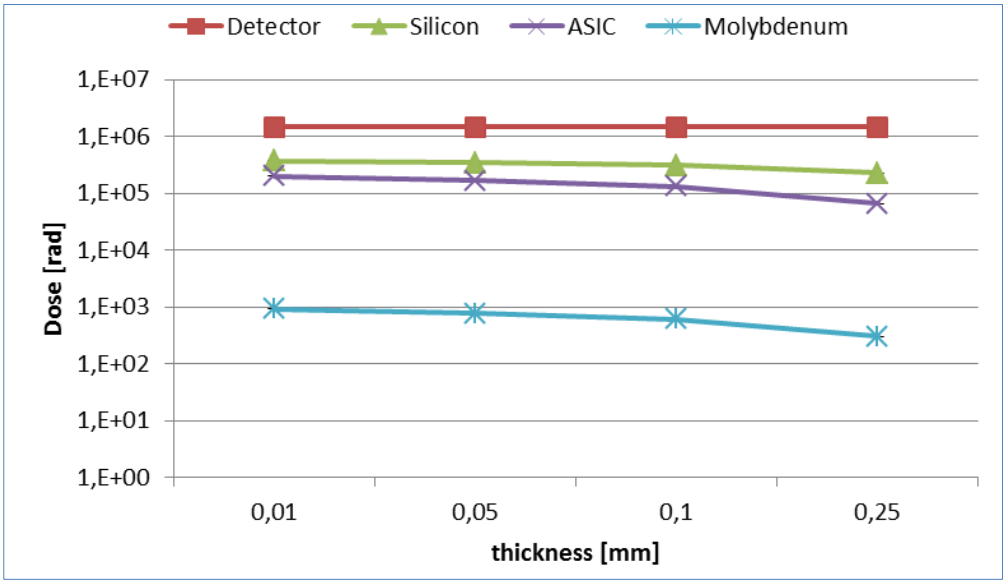

Figure 13. *Radiation dose from 12 keV X-rays accumulated in different components for a silicon interconnect*

3 Conclusion

In conclusion, the simulations have shown that LPD ASICs below a tantalum or tungsten layer of a thickness of approximately 125 µm or more will be well shielded from the incident X-rays.

It was further found that such layers will result in fluorescence emission and backscattering onto the detector. These additional events will result in a larger gain for pixels above the layer—an offset that can be corrected for during calibration.

This fluorescence emission also introduces an additional uncertainty on top of the Poisson uncertainty of the incident emission, which will at maximum reach ~ 0.8% in terms of incident photons, corresponding to ~ 11.5% of the Poisson uncertainty, for low photon counts. For high photon counts, it is consistently below 0.02%. Accordingly, it can likely be neglected regardless of the incident flux.

It should be pointed out that these simple simulations did not estimate the effects of radiation passing through the interposer and then scattering onto the ASIC from the underlying molybdenum layer. Similarly, the true pixel structure and 3D structure of the detector was not taken into account. In order to further investigate the effects with a more detailed simulation, which takes this into account, the simulation code has been supplied to the LPD collaboration.

References

[1] S. Agostinelli et al.:“Geant4—a simulation toolkit”, Nuclear Instruments and Methods in Physics A **503**, 3, 250–303 (2003)

[2] K. Amako et al.: ”Geant4 developments and applications”, IEEE Transactions on Nuclear Sciences **53**, 1, 270–278 (2006)

[3] F. Lei et al.: “MULASSIS: A Geant4-based multilayered shielding simulation tool”, IEEE Transactions on Nuclear Science **9**, 6, 2788–2793 (2002)

[4] N. Meidinger et al.: “Development of the focal plane PNCCD camera system for the X-ray space telescope eROSITA”, Nuclear Instruments and Methods in Physics Research Section A **624**, 2, 321–329 (2010)